Flexible Conjugated Polyelectrolyte Solutions: A Small Angle Scattering Study

P. Vallat, J.-M. Catala, M. Rawiso, and F. Schosseler*

Institut Charles Sadron, 6 rue Boussingault, 67083 Strasbourg Cedex, France

Received December 22, 2006; Revised Manuscript Received February 15, 2007

ABSTRACT: The aqueous solutions of a fully neutralized flexible conjugated polyacid, the poly(3-thiophene sodium acetate) (P3TNaA), are studied by small angle scattering techniques, as a function of polymer concentration, molecular weight and added salt concentration. The characteristic polyelectrolyte scattering peak obeys the predictions of the isotropic model, in good agreement with the behavior of saturated polyelectrolyte solutions. Despite the presence of irreversible aggregates formed during the synthesis, no further aggregation occurs in solution whatever the polymer or added salt concentration. Thus, these conjugated polyelectrolytes remain hydrosoluble and well-dispersed when the electrostatic repulsion is screened, probably due to their small bare persistence length that prevents large dispersion forces in the undoped state.

1. Introduction

Conjugated polymers have generated a large amount of work in the past two decades and have proven to be promising materials in different fields including nanoconductors, field-effect transistors, bio- and chemosensors, photovoltaics.[1] However the extended π electron delocalization along the polymer backbone makes such polymers insoluble and considerable efforts have been devoted to the modification of existing monomers to increase their solubility without compromising the delocalization of the π electrons. One interesting route to this goal is the grafting of side groups carrying electrical charges.[2,3] The obtained conjugated polyelectrolytes become then water-soluble or water-dispersible and new more environment-friendly processing routes can then be envisioned for these materials. Moreover this new feature opens interesting applications as biosensors or as chemosensors in aqueous solutions.[4]

For these applications the understanding of the polyions conformation as a function of physicochemical parameters is critical. As an example, the efficiency of photoluminescence quenching in conjugated polymers appears to depend on the extension of the chains in solution,[5−7] conditioning the sensitivity of bio- and chemosensors based on this phenomenon. However only few papers[8−17] have reported on the structure of aqueous solutions of conjugated polyelectrolytes as revealed by scattering techniques.

Recent reports have focused on the structure of aqueous solutions of conjugated polyelectrolytes with a rather rigid backbone, like derivatives of poly(*p*-phenylene)[8,11−17] or poly(phenylenevinylene) (PPV).[9,10] In the first case, either hexagonal ordering of aggregated cylinders[8,11,12] or well-dispersed chains[13−17] were obtained, depending on the nature of the side chains. In the second case, the experimental results have shown a broad scattering peak in the small-angle neutron scattering curves. The behavior of this maximum as a function of polyelectrolyte concentration and added salt concentration[9,10] is consistent with the isotropic model[18−20] of polyelectrolyte solutions. In all these studies the polyelectrolytes are salts of strong acid groups and their effective charge is fixed at the Manning−Oosawa value.[21−24]

This paper is part of a series dealing with the properties of poly(3-thiophene sodium acetate) (P3TNaA) solutions. In contrast with the previously studied conjugated polyelectrolytes, undoped poly(thiophene) derivatives are known to have a rather low persistence length, about 2.2 nm for poly(3-butyl thiophene) in nitrobenzene at 65 °C[25] and about 2.4 nm for poly(3-hexyl thiophene) in tetrahydrofuran at room temperature.[26] Moreover, since charges are brought by carboxylic groups the degree of ionization can be controlled through the pH.

The synthesis of poly(3-thiophene acetic acid) has been previously described by Kim et al.[27] Introducing slight modifications in their method we obtained P3TNaA chains with varying degree of polymerization DP, $45 \leq DP \leq 125$, and reasonable polydispersity index close to 2. In this paper, the aqueous solutions of fully neutralized chains are studied by means of small-angle neutron and X-ray scattering techniques, as a function of polyelectrolyte concentration, molecular weight, and added salt concentration. A forthcoming contribution will deal with the effects of varying the charge of the chains.[28]

2. Experimental Part

2.1 Synthesis and Characterization of poly(3-thiophene methyl acetate) (P3TMA). The poly(thiophene-3-acetic acid) (P3TAA) is obtained through saponification of the ester groups of P3TMA chains, first synthesized by an oxidative-coupling polymerization,[29,30] as proposed by Kim et al.[27] The 3TAA monomer was purchased from Acros and first esterified into 3TMA.[27] Some slight modifications to the original procedure were found to increase the reproducibility of the synthesis and the yield of the precipitated polymer, and helped us to obtain large quantities of rather high molecular weight P3TMA. With our procedure, this yield is about 35% whereas it was not larger than 12% with the original procedure. Our modifications together with the details of the methods of characterization of the samples are described in the Supporting Information (SI).

Samples were fractionated by Soxhlet extraction, successively by different solvents to obtain fractions with increasing molecular weights, as described in the Supporting Information. ^{1}H and ^{13}C NMR analysis showed no significant difference in the regioregularity of the different fractions that can be considered as regio-irregular samples. Table 1 gives the weight-average molecular weights and polydispersities of the main fractions used in the scattering experiments.

2.2. Synthesis and Characterization of Poly(3-thiophene sodium acetate). The saponification of the P3TMA was performed under milder conditions than those used in the work by Kim et

* Corresponding author. E-mail: schossel@ics.u-strasbg.fr.

10.1021/ma062942f CCC: $37.00
Published on Web 04/11/2007

Table 1. Characteristics of the P3TMA Fractions[a]

SEC		
PS calibration		P3TMA calibration
M_w	M_w/M_n	M_w
5800	1.5	10 000
7000	1.5	11 900
24 000	2.2	41 000

[a] Relative errors on M_w values are estimated about 0.2.

al.[27] (see SI for the details). After the saponification, the excess of NaOH was neutralized by HCl and the samples were carefully dialyzed, which yielded a partial acidification of the polyelectrolyte chains since poly(3-thiophene acetic acid) is a weak polyacid. Therefore, an aliquot of the solution was titrated forth and back with NaOH and HCl to determine the true neutralization degree of the polymer in the dialyzed solution. The appropriate amount of NaOH was then added to the batch solution to recover fully neutralized P3TNaA chains that were isolated by freeze-drying. The water content of the final red-orange solid was determined by thermogravimetric analysis to be about 10% and was taken into account for the preparation of solutions. The final product was stored in the dark, under argon, at room temperature.

^{1}H NMR spectrum of the polyelectrolyte in D_2O indicated that the saponification was complete and yielded one ionizable group per monomer. UV−visible absorption spectroscopy showed a broad maximum in the absorbance located at $\lambda_{max} = 435$ nm and a peak height $\epsilon_{max} = 6600$ cm^{-1} M^{-1}. Field-flow-fractionation gave a value of the weight-average degree of polymerization of the polyelectrolyte chains in good agreement with that of the P3TMA precursors, confirming that no significative chain degradation occurred during the saponification with our experimental conditions.

2.3. Sample Preparation. The solutions were prepared by weighing the appropriate amount of polymer in ultrapure water (Millipore) or in D_2O (Eurisotop, 99,9%), depending on the scattering technique used. They were heated at 50 °C for 2 h and prepared at least 2 days before use. In the case of filtrated solutions, the final concentration was measured by UV−visible absorption spectroscopy.

2.4. Small-Angle Neutron Scattering (SANS). Different experimental runs were conducted on spectrometer PAXY (Laboratoire Léon Brillouin, Saclay, France). Samples were prepared as described above. Measurements were carried out in standard Hellma cells built from two quartz disks separated by an annular quartz spacer with a thickness of 2.5 mm. Standard data treatment was performed and involved correction for transmission and thickness, normalization by the intensity scattered from 1 mm of H_2O, and background subtraction (incoherent scattering from polymer and solvent scattering). Incoherent scattering level for each sample was obtained from interpolation through a set of measurements performed on mixtures of D_2O/H_2O with different compositions. The interpolated value was calculated on the basis of the H content in the sample. The data were put on an absolute scale by using the incoherent scattering cross section of 1 mm of H_2O.

2.5. Small-Angle X-ray Scattering (SAXS). Small-angle X-ray scattering experiments have been performed with spectrometers ID02 and D2AM (European Synchrotron Research Facility, Grenoble). Quartz capillary (ID02) or sample holder (D2AM) with mica windows were used and the sample thickness was kept to 1 mm. Data treatment involved correction for incident photon flux and for sample transmission, and subtraction of the intensity scattered from pure water, free counterions, and empty cell.

3. Results and Discussion

3.1. Without Added Salt. Typical SANS intensity curves $I(q)/C$ scattered from P3TNaA solutions are shown in Figure 1 for chains with DP = 45 and DP = 125. Here C is the polymer concentration and q is the scattering vector defined as $q = 4\pi/\lambda \sin(\vartheta/2)$, with λ the incident wavelength and ϑ the scattering angle. In most cases, the concentration is the nominal one, as given by the amount of dry polymer dissolved in the solvent. For the highest concentrations, however, the nominal concentration of the filtered solutions can be about 15% larger than the concentration measured by UV−visible absorption spectroscopy and the latter one was used instead, in order to collapse together the scattering curves in the high q range, where the intensity should be proportional to the concentration of polymer units since intermolecular correlations become negligible.

The scattering curves exhibit two prominent features: a strong upturn at low q values and a peak at intermediate q values. The upturn intensity appears to be proportional to the polymer concentration and its level is comparable for chains with different DPs (Figure 1). Its scattering behavior can be described empirically by a power law with an exponent close to −3 and its amplitude seems to be more prominent than for usual polyelectrolyte solutions for which upturns are often not observed for q values larger than 0.01 Å^{-1}. As an example, a similar power law behavior with a smaller exponent about −2.7 has been reported for the upturn intensity measured in aqueous solutions of quaternized poly(2-vinylpyridine).[31] In this case, the upturn intensity is thought to be linked in some way to the so-called slow relaxation mode measured in polyelectrolyte solutions by dynamic light scattering experiments. However a consensus about the physical meaning of this slow mode has not been reached as yet.[32] In our case the features of the upturn intensity suggest that it could be associated with the presence of aggregates with moderate size, constant density and rough surface: fractal aggregates would correspond to a power law with an exponent smaller than −3 while sharp and smooth interfaces would contribute with a Porod law decay and an exponent of −4.

The scattering peak appears to be slightly better resolved for the smaller chains and, for both DP values, its position q^* shifts to larger values as the polymer concentration increases (Figure 2). Two concentration regimes can be distinguished: (i) at high polymer concentration, q^* is independent of the molecular weight of the chains and its variation is consistent with a power law $q^* \sim C^{1/2}$; (ii) at smaller polymer concentrations, the position of the peak depends on the molecular weight and its variation is consistent with $q^* \sim C^{1/3}$.

These variations are those expected for the so-called polyelectrolyte peak, as predicted by the scaling laws within the isotropic model[18−20] and confirmed by experiments on solutions of polyelectrolytes with a saturated backbone.[31−37] The high concentration regime is the semidilute one:[38] the polymer chains are overlapping and the scattering peak reflects the correlation hole due to the strong repulsion between electrostatic blobs and the small osmotic compressibility of the solutions.[18] In the low concentration regime, the peak scales like the inverse of the average distance between dilute charged objects. The transition between these two regimes occurs for the overlap concentration $C^* \sim N/R^3$, where N and R are the DP and a characteristic dimension of the chains, respectively. For polyelectrolyte chains extended by long range repulsive interactions, $R \sim N$ and therefore $C^* \sim N^{-2}$.[18] This power law has been confirmed through the compilation of experimental results obtained on solutions of poly(styrene sodium sulfonate) (NaPSS).[39] Our experimental values for C^* as a function of degree of polymerization fit fairly well in the data compilation for NaPSS (Figure 3).

It can be emphasized that, as for NaPSS solutions, a noticeable difference appears between q^* values measured by SANS and SAXS at high concentration. This has been explained

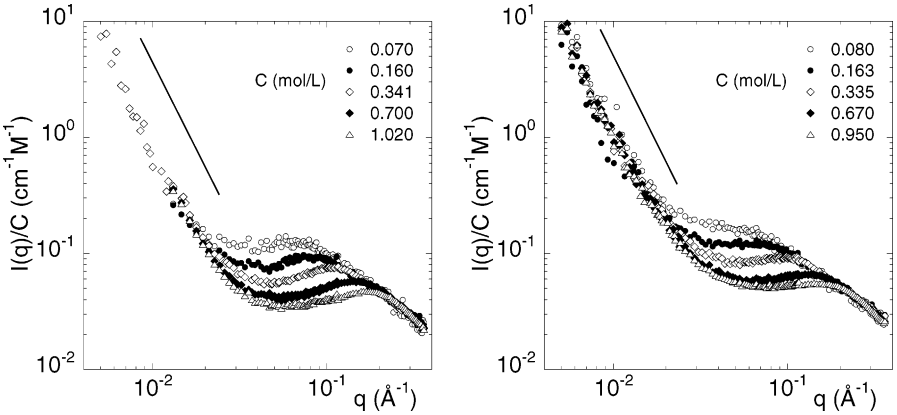

Figure 1. Evolution with polymer concentration of the SANS scattering intensity per monomer: (a) DP = 45; (b) DP = 125. The straight lines correspond to a q^{-3} power law decay.

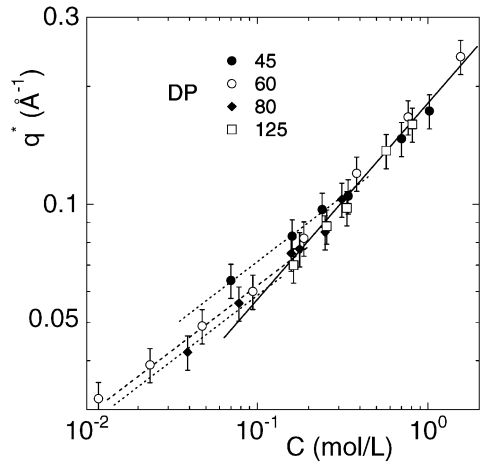

Figure 2. Variation of the peak position q^* as a function of polymer concentration. The continuous and dotted lines have slopes of $^1/_2$ and $^1/_3$ in the semidilute and dilute regimes, respectively. Relative errors on q^* are estimated about 0.10 from the plots in Figure 1.

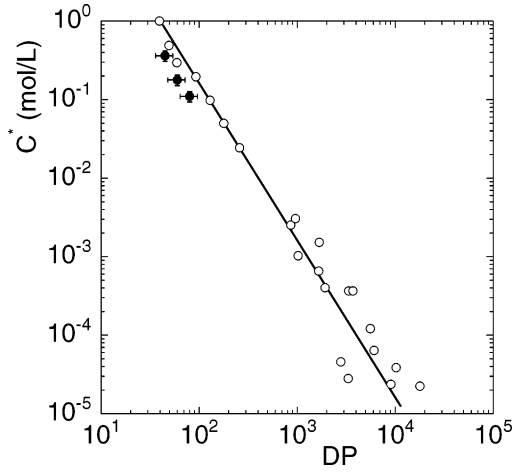

Figure 3. Comparison of C^* values obtained for NaPSS (opened symbols) and for P3TNaA (closed symbols). Data for NaPSS come from the compilation given in ref 39. Relative errors in our experiments are estimated to be 0.2 on DP values and 0.15 on C^* values determined from the data in Figure 2. The continuous line corresponds to a power law with exponent −2.

as a subtle effect arising from the difference of contrasts in the two techniques:[40] in SANS, the contrast is provided by the atoms in the backbone relative to the solvent while in SAXS the contrast arises mainly from the Na counterions condensed around the backbone. Thus, in SANS, the form factor of the chains is locally, at high q values, that of a filled cylinder instead of an empty cylinder in SAXS. Intermolecular correlations mix increasingly with the details of the local form factor as their characteristic length scale decreases upon concentration increase and q^* values measured by SANS and SAXS split. As a consequence, the observed power laws differ. The same effect is at work here where a further complication arises from the S atoms contributing significantly more than the other atoms in the SAXS experiments. As a consequence, for concentrations larger than 0.2 mol/L, we observe a scaling behavior that depends on the scattering technique: $q^* = 0.151C^{0.43}$ (SAXS) instead of $q^* = 0.180C^{0.5}$ (SANS). On the other hand, SANS experiments are extremely difficult in the dilute regime where synchrotron SAXS is more reliable. Therefore, the data in Figure 2 are obtained from SAXS experiments for concentrations below $C = 0.1$ mol/L and from SANS above this limit.

Finally the correlation length $\xi = 2\pi/q^*$ of solutions of flexible polyelectrolyte chains in the weak coupling limit is expected to follow the scaling law:[41]

$$\xi \approx f^{-2/7}(l_B/b)^{-1/7}(bC)^{-1/2} \quad (1)$$

where f is the degree of ionization, l_B the Bjerrum length, and b the length of the monomer. For chains in the strong coupling limit, f should be replaced by the effective charge f_{eff} calculated by Manning−Oosawa theory.[21−24] Thus, for fully ionized chains ($f = 1$), f_{eff} is pinned at b/l_B and

$$\xi \approx (l_B/b)^{1/7}(bC)^{-1/2} \quad (2)$$

The compilation of published data has indeed shown[40] that the position of the maximum in the scattering curves of polyelectrolytes in the semidilute regime follows a master curve when q^* is plotted as a function of $2\pi/\xi$, with ξ calculated by eq 2. Figure 4 shows the corresponding data for the present samples together with the data compilation published previously.[40] For the P3TNaA, b was taken as $b = 0.38$ nm. The data for P3TNaA collapse reasonably well on the same master line as other polyelectrolytes with a saturated backbone. A better agreement with the compiled data would be obtained with the value $b = 0.23$ nm, which appears, however, to be rather unrealistic from molecular models.

In the isotropic model, the intensity per monomer at $q = q^*$ is predicted to scale as $I(q^*)/C \sim C^{-1/2}$,[19,20] in agreement with the experimental behavior of flexible saturated polyelectrolyte solutions in the semidilute regime.[37,42] The same behavior was reported recently for the rather rigid conjugated chains based on PPV.[10] Figure 5 shows that solutions of P3TNaA exhibit the same trend as the semidilute regime is entered. However it

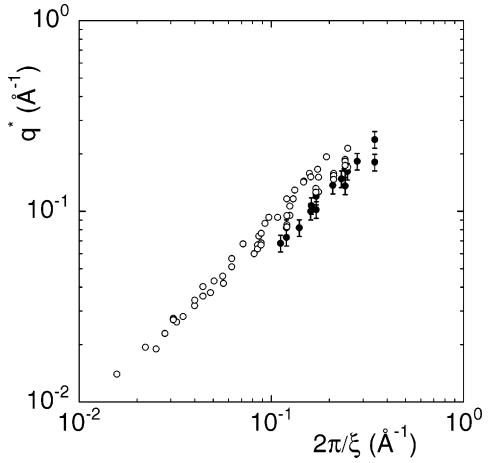

Figure 4. Master curve q^* vs $2\pi/\xi$ where ξ is calculated by eq 2 in the text. Closed symbols: our data for P3TNaA (errors bars as in Figure 2); Open symbols: compilation of published experimental data with details given in ref 40.

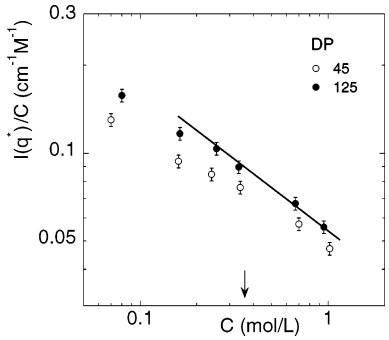

Figure 5. Evolution of the scattering intensity per monomer at the maximum $I(q^*)/C$ as a function of polymer concentration. Relative errors are estimated about 0.05. The continuous line has a slope $-1/2$. The arrow indicates the C^* value for DP = 45 (Figures 2, 3). For DP = 125, C^* could not be determined and should be about 0.04 mol/L from the extrapolation of the data in Figure 3.

seems that $I(q^*)/C$ is still slightly dependent on the molecular weight even in the semidilute regime. This difference could be due to a contribution of the upturn intensity but it was also observed for NaPSS solutions[37] for which the upturn intensity is present at smaller q values than in the present system. This suggests that the crossover transition between the dilute and the semidilute regime could span a larger concentration range for the scattering intensity at the peak than for the position of this peak.

3.2. With Added Salt. We have increased the screening of electrostatic repulsions by adding a monovalent salt, NaCl. All SANS experiments have been performed at a fixed polymer concentration $C = 0.34$ mol/L. The total ionic strength is defined as $I = (f_{\text{eff}}C + 2C_s)/2$, where $f_{\text{eff}} = b/l_B = 0.54$ and C_s is the molar salt concentration. The ratio I/I_0 measures the increase of the screening relatively to that arising from the free counterions, $I_0 = f_{\text{eff}}C/2 = 0.092$ mol/L. The Debye screening length l_D is then simply given by $l_D = l_{D,0}(I/I_0)^{-1/2}$ where $l_{D,0} = (8\pi l_B I_0)^{-1/2} \approx 10.1$ Å.

As we increased the salt concentration up to $C_s = 1$ mol/L ($1 \leq I/I_0 \leq 12$), the solutions remained optically clear, and we never observed a phase separation. The effects on the total structure function are classical (Figure 6) as far as the polyelectrolyte peak is concerned: the peak shifts to smaller q values for moderate quantities of added salt and finally disappears for higher salt concentrations ($C_s > 0.1$ mol/L). Actually, this behavior corresponds to a peak moving in the opposite direction

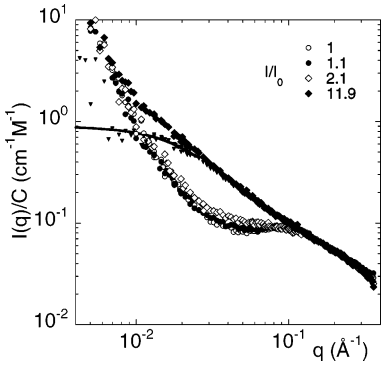

Figure 6. Evolution of SANS scattering intensity curves with the amount of added salt, $C = 0.34$ mol/L. Small triangles correspond to the intensity of the sample at $I/I_0 = 11.9$ once a power law fitted to the upturn intensity measured at low salt concentration has been subtracted. This remaining contribution can be fitted by a Lorentzian curve (continuous line).

for the intermolecular contribution to the total structure function.[43]

One interesting feature is the effect of salt addition on the upturn intensity. For a conjugated polyelectrolyte solubilized by electrostatic repulsions, one would expect that the screening of these interactions would enhance the formation of aggregates as the overall solvent quality becomes poorer. This was the observed behavior for neutral polydiacetylene (P4BCMU) solutions where the solvent quality was varied through the temperature:[44] side-by-side aggregation due to van der Waals interactions was revealed by a strong increase of the small q intensity as the solvent quality became poorer. For a rigid conjugated polyelectrolyte based on PPV the opposite behavior was observed: salt addition was found to decrease the upturn intensity at small q values.[10] In the present case, these effects were never observed and the upturn intensity remained at the same level as in the absence of added salt, whatever the molecular weight of the chains. This can be checked for the sample with the higher salt concentration by subtracting a power law with exponent -3 fitted to the upturn intensity measured at low salt concentration. The remaining intensity (Figure 6, triangles) has a Lorentzian shape with a correlation length about 40 Å (Figure 6, continuous line), as can be expected for a semidilute polyelectrolyte solution at this concentration with an excess of added salt.

4. Conclusions

The structure of the aqueous solutions of P3TNaA, a flexible conjugated polyelectrolyte, has been studied by using small angle scattering techniques as a function of polymer concentration, molecular weight, and added salt concentration.

The small angle intensity scattered from P3TNaA solutions can be satisfactorily described by the isotropic model for polyelectrolyte solutions and the associated scaling laws. Thus, these fully neutralized conjugated polyelectrolytes exhibit the same overall behavior as other flexible polyelectrolytes with a saturated backbone.

The main difference between saturated and conjugated chains lies in the strong upturn scattering that arises at larger q values for the conjugated polymers than usually reported for saturated chains. Remarkably, the upturn intensity appears to be proportional to polymer concentration, to depend very weakly on the molecular weight, and to be independent of the added salt concentration. Moreover, upon monovalent salt addition, we do not observe a phase separation for these fully charged chains. All these features indicate that in the present case the dominant

contribution to the upturn intensity is linked to irreversible aggregates that are formed during polymer preparation. In particular, their amount increases when an acid route is used to recover the polymer chains instead of the salt route mainly used in this study (see SI). This suggests that both the polymerization at the solid−liquid interface and the subsequent saponification are critical steps where these aggregates can form. Significant differences are observed with the behavior of rigid PPV based polyectrolytes where the upturn intensity disappears in the presence of added salt. Apart from these aggregates, fully neutralized P3TNaA chains remain globally hydrophilic whatever the salt concentration: the dispersion forces linked to the delocalized π electrons do not induce aggregation when the electrostatic repulsion is screened. This is likely due to the small natural persistence length of the polythiophene backbone.

Acknowledgment. We thank J.-P. Lamps for his help at various steps along the synthesis, A. Rameau, C. Foussat, and J. Selb for performing the SEC and FFF characterizations for us, and J. Combet and Y. Frère for fruitful discussions. We are also grateful to our local contacts at LLB, F. Boué, and at ESRF, T. Narayanan and C. Rochas, for helpful assistance during the experiments. P.V. benefited from a thesis grant jointly funded by Région Alsace and CNRS. Part of this work was funded by an ACI grant from the French Ministry of Research.

Supporting Information Available: Text detailing the synthesis and characterization of the samples, figures showing size exclusion chromatograms for P3TMA, variation with molecular weight of the peak position in the UV−visible absorption spectra of P3TMA in THF, and the titration curve of P3TAA in H_2O, and a table giving characteristics of the P3TMA fractions. This material is available free of charge via the Internet at http://pubs.acs.org.

References and Notes

(1) Heeger, A. J. *J. Phys. Chem. B* **2001**, *105*, 8475.
(2) Bhattacharjee, H. R.; Preziosi, A. F.; Patel, G. N. *J. Chem. Phys.* **1980**, *73*, 1478.
(3) Patil, A. O.; Ikenoue, Y.; Wudl, F.; A. J. Heeger, A. J. *J. Am. Chem. Soc.* **1987**, *109*, 1858.
(4) Chen, L.; McBranch, D. W.; Wang, H.; Helgeson, R.; Wudl, F.; Whitten, D. G. *Proc. Natl. Acad. Sci. U.S.A.* **1999**, *96*, 12287.
(5) Wang, J.; Wang, D.; Miller, E. K.; Moses, D.; Bazan, G. C.; Heeger, A. J. *Macromolecules* **2000**, *33*, 5153.
(6) Xu, Q.-H.; Gaylord, B. S.; Wang, S.; Bazan, G. C.; Moses, D.; Heeger, A. J. *Proc. Nat. Acad. Sci. U.S.A.* **2004**, *101*, 11634.
(7) Cabarcos, E. L.; Carter, S. A. *Macromolecules* **2005**, *38*, 10537.
(8) Rulkens, R.; Wegner, G.; Thurn-Albrecht, T. *Langmuir* **1999**, *15*, 4022.
(9) Wang, D.; Lal, J.; Moses, D.; Bazan, G. C.; Heeger, A. J. *Chem. Phys. Lett.* **2001**, *348*, 411.
(10) Wang, D. L.; Moses, D.; Bazan, G. C.; Heeger, A. J.; Lal, J. *J. Macromol. Sci., Pure Appl. Chem.* **2001**, *38*, 1175.
(11) Bockstaller, M.; Köhler, W.; Wegner, G.; Fytas, G. *Macromolecules* **2001**, *34*, 6353.
(12) Kroeger, A.; Belack, J.; Larsen, A.; Fytas, G.; Wegner, G. *Macromolecules* **2006**, *39*, 7098.
(13) Guilleaume, J.; Blaul, J.; Wittemann, M.; Rehahn, M.; Ballauff, M. *J. Phys.: Cond. Matter* **2000**, *12*, A245.
(14) Guilleaume, B.; Blaul, J.; Ballauf, M.; Wittemann, M.; Rehahn, M.; Goerigk, G. *Eur. Phys. J. E.* **2002**, *8*, 299.
(15) Ballauf, M.; Blaul, J.; Guilleaume, B.; Rehan, M.; Traser, S.; Wittemann, M.; Wittmeyer, P. *Macromol. Symp.* **2004**, *211*, 1.
(16) Patel, M.; Rosenfeldt, S.; Ballauf, M.; Dingenouts, N.; Pontoni, D.; Narayanan, T. *Phys. Chem. Chem. Phys.* **2004**, *6*, 2962.
(17) Ballauf, M.; Jusufi, A. *Colloid Polym. Sci.* **2006**, *284*, 1303.
(18) de Gennes, P. G.; Pincus, P. A.; Velasco, R. M.; Brochard, F. *J. Phys. Paris* **1976**, *37*, 1461.
(19) Koyama, R. *Macromolecules* **1984**, *17*, 1594.
(20) Koyama, R. *Macromolecules* **1986**, *19*, 178.
(21) Oosawa, F. *Biopolymers* **1968**, *6*, 135.
(22) Oosawa, F. *Polyelectrolytes*; Marcel Dekker: New York, 1971.
(23) Manning, G. *J. Chem. Phys.* **1969**, *51*, 924.
(24) Manning, G. S. *Polyelectrolytes*; Sélégny, E.; Mandel, M.; Strauss, U. P., Eds.; D. Reidel: Dordrecht, The Netherlands, 1974.
(25) Aimé, J.-P.; Bargain, F.; Schott, M.; Eckhardt, H.; Miller, G. G.; Elsenbaumer, R. L. *Phys. Rev. Lett.* **1989**, *62*, 55.
(26) Heffner, G. W.; Pearson, D. S. *Macromolecules* **1991**, *24*, 6295.
(27) Kim, B.; Chen, L.; Gong, J. P.; Osada, Y. *Macromolecules* **1999**, *32*, 3964; **2000**, *33*, 648.
(28) Manuscript in preparation.
(29) Yoshino, K.; Hayashi, S.; Sugimoto, R. *Jpn. J. Appl. Phys.* **1984**, *23*, L899.
(30) Sugimoto, R.; Takeda, S.; Gu, H. B.; Yoshino, K. *Chem. Express* **1986**, *1*, 635.
(31) Förster, S.; Schmidt, M.; Antonietti, M. *Polymer* **1990**, *31*, 781.
(32) For a review see Förster, S; Schmidt, M. *Adv. Polym. Sci.* ***1995****, 120, 51*.
(33) Cotton, J.-P.; Moan, M. *J. Phys., Lett.* **1976**, *37*, L75.
(34) Nierlich, M.; Williams, C. E.; Boué, F.; Cotton, J.-P.; Daoud, M.; Farnoux, B.; Jannink, G.; Picot, C.; Moan, M.; Wolf, C.; Rinaudo, M.; de Gennes, P. G. *J. Phys. (Paris*) **1979**, *40*, 701.
(35) Drifford, M.; Dalbiez, J.-P. *J. Phys. Chem.* **1984**, *88*, 5368.
(36) Ise, N.; Okubo, T.; Kunugi, S.; Matsuoka, H.; Yamamoto, K.; Ishii, Y. *J. Chem. Phys.* **1984**, *81*, 3294.
(37) Kaji, K.; Urakawa, H.; Kanaya, T.; Kitamaru, R. *J. Phys. (Paris*) **1988**, *49*, 993.
(38) de Gennes, P. G. *Scaling Concepts in Polymer Physics*; Cornell University Press: Ithaca, NY, 1979.
(39) Boris, D. C.; Colby, R. H. *Macromolecules* **1998**, *31*, 5746.
(40) Combet, J.; Isel, F.; Rawiso, M.; Boué, F. *Macromolecules* **2005**, *38*, 7456.
(41) Dobrynin, A. V.; Colby, R. H.; Rubinstein, M. *Macromolecules* **1995**, *28*, 1859.
(42) Jannink, G. *Makromol. Chem. Symp.* **1986**, *1*, 67.
(43) Nishida, K.; Kaji, K.; Kanaya, T.; Shibano, T. *Macromolecules* **2002**, *35*, 4084.
(44) Rawiso, M.; Aimé, J.-P.; Schott, M.; Fave, J.-L.; Schmidt, M.; Muller, G.; Wegner, G. *J. Phys. (Paris*) **1988**, *49*, 861.

MA062942F